

1-1-2016

Accessing Spin-Crossover Behaviour In Iron(II) Complexes Of N-Confused Scorpionate Ligands

James R. Gardinier

Marquette University, james.gardinier@marquette.edu

Alexander Richard Treleven

Marquette University

Kristin J. Meise

Marquette University

Sergey Lindeman

Marquette University, sergey.lindeman@marquette.edu

Accessing Spin-Crossover Behaviour In Iron(II) Complexes Of N- Confused Scorpionate Ligands^{†‡}

James R. Gardinier

*Department of Chemistry, Marquette University,
Milwaukee, WI*

Alex R. Treleven

*Department of Chemistry, Marquette University,
Milwaukee, WI*

Kristin J. Meise

*Department of Chemistry, Marquette University,
Milwaukee, WI*

Sergey V. Lindeman

*Department of Chemistry, Marquette University,
Milwaukee, WI*

The first examples of a class of N-confused tris(pyrazolyl)methane 'scorpionate' ligands have been prepared. The magnetic properties of their iron(II) tetrafluoroborate complexes are dictated by changing one substituent per ligand rather than three as is typical for normal scorpionate ligands.

Investigations into the magnetic properties of d^4 – d^7 metal complexes have been partly inspired by the intoxicating allure of developing molecular switches or other innovative technologies that could exploit spin crossover (SCO) behaviour.¹ For instance, SCO complexes have been employed in thermochromic displays,² show potential as sensors,³ MRI contrast agents⁴ and, most recently, in spintronics⁵ and various molecular electronics applications.⁶ Among the sundry of complexes that exhibit SCO behaviour, iron(II) scorpionates (tris(pyrazolyl)borates,⁷ tris(pyrazolyl)methanes,⁸ and related analogues⁹) are garnering increased interest because of the simplicity of their syntheses, their high stability, and diverse magnetic behaviour. Notably Trofimenko first showed that $\text{Fe}[\text{HB}(\text{pz})_3 = \text{Tp}]_2$ (pz = pyrazol-1-yl) underwent a spin-state change from $S = 0$ to $S = 2$ above room temperature in solution and the solid state.¹⁰ In the solid state, the SCO behaviour of the first heating cycle differs from other heating and cooling cycles because of an irreversible phase change on heating from a metastable tetragonal crystal system to a more stable monoclinic system maintained thereafter.¹¹ This property can be exploited for the development of read-only memory devices.¹² The related FeTp^*_2 (Tp^* = tris(3,5-dimethylpyrazol-yl)borate) is high spin in solution but undergoes spin crossover and is low spin at 78 K and below.¹³ The iron(II) complexes of charge-neutral scorpionates such as $\text{Tpm} = [\text{HC}(\text{pz})_3]$ or $\text{Tpm}^* = [\text{HC}(\text{pz}^*)_3]$ (pz^* = 3,5-dimethylpyrazol-1-yl) also show highly variable magnetic behaviour. The compounds $[\text{Fe}(\text{Tpm})_2](\text{X})_2$ ($\text{X} = \text{PF}_6$,¹⁴ ClO_4 ,¹⁵ NO_3 ,¹⁶ BF_4 ¹⁷) are low spin at room temperature but undergo SCO above 300 K. $[\text{Fe}(\text{Tpm}^*)_2](\text{BF}_4)_2$ is high spin at room temperature but undergoes an abrupt SCO at 206 K in the solid to give a sample with 50% low-spin sites that originates from a crystallographic phase transition.¹⁸ Also, one of the two polymorphs of $[\text{Fe}(\text{Tpm})(\text{Tpm}^*)](\text{BF}_4)_2$ undergoes an abrupt SCO with $T_{1/2}$ (50% LS) at 228 K whereas the other with less efficient solid packing has a gradual spin crossover with $T_{1/2}$ near 300 K.¹⁹ Thus, the SCO capabilities of iron(II) scorpionates are profoundly affected by the nature of the 3-pyrazolyl substituents near the metal centre and by their crystal packing. In numerous studies on iron(II) scorpionates, those with pyrazolyl substituents larger than methyls typically either give heteroleptic species²⁰ or, if homoleptic,²¹ remain HS, as nicely summarized recently: "...any substituents in the 3-position that are much larger than a methyl destroy any hope of observing spin state

crossover behaviour and essentially lock the complex into the HS form".²² While the above statement seems hyperbole, Fe[HB(3-cypropylpz)₃]₂ is the only case of a bulkier Tp^R iron(II) complex to show SCO.⁷ We sought a ligand design that would allow ready (perhaps "on demand") modification of pyrazolyl groups near the metal centre in order to discover new examples of SCO behaviour in scorpionates with bulkier pyrazolyls and to extend the current capabilities of scorpionates as supporting ligands. To that end, we have developed the first of a class of scorpionates whereby one of the pyrazolyl rings is connected to the central sp³-carbon in an unusual fashion, by carbon rather than nitrogen (Fig. 1, left). We term these new ligands N-confused scorpionates in analogy to N-confused porphyrins.

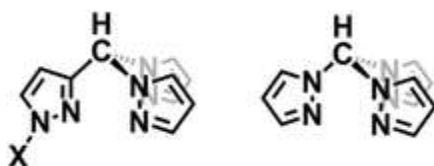
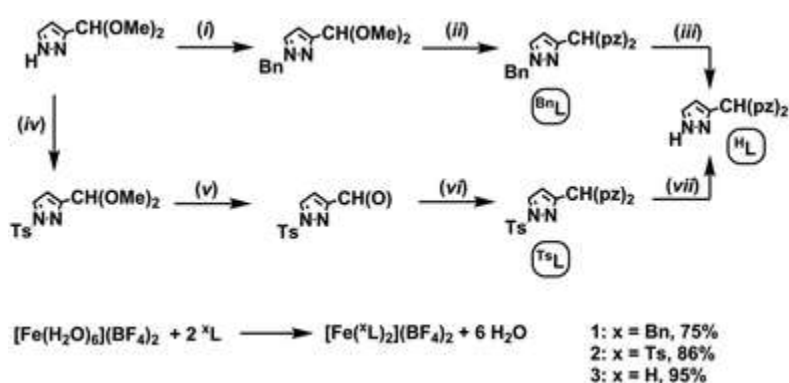


Fig. 1 Left: N-Confused tris(pyrazolyl)methane derivatives reported here (X = H, CH₂C₆H₅ = Bn, p-SO₂C₆H₄CH₃ = Ts). Right: Normal tris(pyrazolyl)methane.

It is envisioned that these new ligands could permit rapid development of sensors or could introduce new vistas for incorporation of scorpionate complexes into 3D networks. In this communication we detail the syntheses of the ligands and the properties of their homoleptic iron(II) complexes. Future reports will detail ligand variants and the implementation of their metal complexes in assemblies, in sensing applications, and in chemical reactions.

The ligands and iron(II) complexes were prepared as summarized in Scheme 1. The ligand syntheses begins with the known²³ H(pz)CH(OMe)₂ that is readily prepared on a 25–50 g scale. The benzyl-protected ligand, ^{Bn}L, is obtained in high yield in two steps that ultimately exploits an acid-catalysed condensation reaction between pyrazole and BnpzCH(OMe)₂. The resulting ^{Bn}L is surprisingly unreactive toward typical benzyl deprotecting agents (various catalytic palladium reagents, H⁺ and/or H₂) but could be oxidatively deprotected in superbasic medium to give very low yields of the protonated ligand ^HL. Attention was then turned to a tosyl-protected analogue, ^{Ts}L, since this species was expected (and found) to be more reliably deprotected under milder conditions. Tosylation of HpzCH(OMe)₂ to give TspzCH(OMe)₂ proceeded smoothly. Unfortunately, acid-catalysed

condensation with pyrazole to give $^{\text{TSL}}$ under various conditions (solvent, neat) was unsuccessful because of competing reactions; Tspz is formed along with a mixture of products including TspzCH(pz)(OMe) and oligo- and polymeric species from self-condensation of HpzCH(OMe)_2 . Thus, the CoCl_2 -catalysed Peterson rearrangement²⁴ between the aldehyde, TspzCH(O) , and S(O)pz_2 was used to give the desired $^{\text{TSL}}$. The compound $^{\text{HL}}$ was obtained in high yield by the reaction between $^{\text{TSL}}$ and aqueous 5 M NaOH. Importantly, all of the reactions described above can be performed on a large (25–50 g) scale without the need for column chromatography, which makes the new ligands easily accessible.



Scheme 1 Preparation of new scorpionates and iron(II) complexes. Key: (i) NaH, BnBr, THF; (ii) 2 Hpz, 5 mol% pTsOH·H₂O, C₆H₆; (iii) KO^tBu, dmsO, O₂; (iv) TsCl, NaOH, CH₂Cl₂; (v) cat. CF₃CO₂H, H₂O, EtOAc; (vi) S(O)pz₂, cat. CoCl₂, THF; (vii) NaOH (aq), THF, 5 min.

The reaction between $[\text{Fe}(\text{H}_2\text{O})_6](\text{BF}_4)_2$ and two equivalents of the appropriate ligand, $^{\text{x}}\text{L}$, in either THF or acetone, gave a precipitate which after drying the under vacuum was found to be solvent-free $[\text{Fe}(\text{ }^{\text{x}}\text{L})_2](\text{BF}_4)_2$ [$x = \text{Bn}$, (**1**), $x = \text{Ts}$, (**2**); $x = \text{H}$, (**3**)] according to elemental analyses. The structure of **3** was determined at 100 K by single crystal X-ray diffraction of very small twinned crystals of **3** grown by slow evaporation of an aqueous solution. As elaborated in the ESI,[‡] the structure is highly disordered (superposition of trans- and cis-isomers and of anion positions) but the metrics of the FeN₆ kernel could be established (Fig. S1[‡]). Most importantly, the average Fe–N bond length (1.968(2) Å) is indicative of LS iron(II) and is in accord with magnetic data below. Unfortunately, despite exhaustive attempts (vide infra), it has not yet been possible to grow suitable

single crystals of solvent-free **1** or **2** for X-ray diffraction analysis. As solids, **1** and **2** are colourless and paramagnetic with μ_{eff} ca. $5.2\mu_{\text{B}}$ at room temperature and below (SQUID magnetometry, Fig. S2 \pm). Complex **3** is a pink solid at room temperature and below but, on heating to about 150 °C, becomes colourless (and reversibly turns pink on cooling). Magnetic measurements over the temperature range 100 K to 400 K (high T limit of the magnetometer, Fig. 2) show **3** is fully LS Fe(II) at ca. 200 K, begins SCO at higher temperatures, but is not fully HS at 400 K. A $T_{1/2}$ (with 50% HS) of 360 K can be estimated from the data, which is similar to ca. 380 K observed for $[\text{Fe}(\text{Tpm})_2](\text{BF}_4)_2$.¹⁷ Complexes **1** and **2** are paramagnetic in room-temperature CD_3CN solution as indicated by the large chemical shift range (+60 to -40 ppm) of resonances and large solution magnetic moment (μ_{eff} ca. $5.2\mu_{\text{B}}$, Evan's method). The electronic spectrum of each (Fig. S3 \pm) gives intense high energy band(s) in the UV-region (ca. $\lambda < 250$ nm, $\bar{\nu} \sim 40\,000$ cm^{-1} , $\epsilon > 20\,000$ $\text{M}^{-1} \text{cm}^{-1}$) for intraligand transitions and a characteristic low-energy ($\bar{\nu} < 13\,000$ cm^{-1}), low-intensity ($\epsilon < 15$ $\text{M}^{-1} \text{cm}^{-1}$) d-d band for the ${}^5\text{T}_{2g} \rightarrow {}^5\text{E}_g$ transition of high-spin iron(II). From average Gaussian fits of the low energy band of several samples, the crystal field splitting Δ for **1** and **2** is $12\,700 \pm 100$ and $11\,700 \pm 100$ cm^{-1} , respectively. These values are comparable to those found for HS Fe(II) complexes $[\text{Fe}(\text{Tpm}^*)_2]^{2+}$ ($12\,500$ – $14\,600$ cm^{-1} , depending on anion)²⁵ or FeTp^*_2 ($12\,700$ cm^{-1}).¹³ The pink solutions of **3** give paramagnetically shifted ${}^1\text{H}$ NMR spectrum [μ_{eff} (295 K) $0.8\mu_{\text{B}}$] indicative of a small portion of HS Fe(II) in solution. As shown in Fig. S4, \pm the electronic spectrum of **3** in CH_3CN at 295 K shows a weak ($\epsilon = 1.6$ $\text{M}^{-1} \text{cm}^{-1}$) d-d band at $\bar{\nu} = 12\,600$ cm^{-1} for a small portion (ca. 10–20%) presumably of HS **3** overlaid with bands for LS **3**. The latter has intense ($\epsilon = 10^3$ $\text{M}^{-1} \text{cm}^{-1}$) bands in the near UV range ($\bar{\nu} = 30\,000$ – $37\,000$ cm^{-1}) for CT transitions as well as two lower-energy, low-intensity d-d bands [λ_{max} 525, 355 nm; $\epsilon = 50, 400$ $\text{M}^{-1} \text{cm}^{-1}$, respectively] for ${}^1\text{A}_{1g} \rightarrow {}^1\text{T}_{1g}$ and ${}^1\text{A}_{1g} \rightarrow {}^1\text{T}_{2g}$ transitions that are similar to other LS Fe(II) scorpionate complexes. Variable temperature studies show that the bands for HS **3** grow in intensity at the expense of those for LS **3** as temperature is raised from 243 K to 343 K (Fig. S4 \pm). VT NMR data over the same temperature range (Fig. S5 and S6 \pm) show an increase in magnetic moment from 0.8 to $1.3\mu_{\text{B}}$ (Evan's), similar to the solid state moment over the same temperature range. From the electronic spectrum, the

crystal field splitting Δ 19 050 cm^{-1} ($B = 714 \text{ cm}^{-1}$) for LS **3** is comparable to 18 700 cm^{-1} for FeTp_2 and 19 200 cm^{-1} for $[\text{Fe}(\text{Tpm})_2](\text{ClO}_4)_2$.^{15,16} These data are in agreement with earlier observations that Δ is about the same for species with similar $\text{Fe}(3,5\text{-R}_2\text{pz})_6$ kernels, regardless of the bridgehead HC or HB of the scorpionate. Overall, comparisons of the data for **3** and related scorpionate derivatives show that the connectivity of the pyrazolyl unit only has a small influence on the ligand field strength; the groups at the β -pyrazolyl positions (3-pyrazolyl or the N1 position of the confused pyrazolyl) have a more prominent influence.

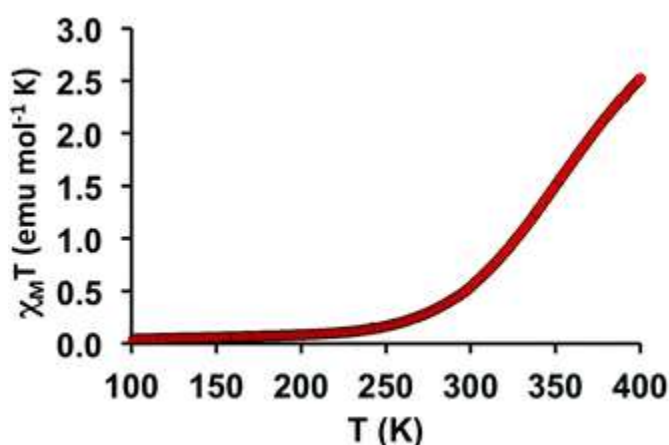


Fig. 2 Temperature dependence of $\chi_M T$ for **3** from SQUID magnetometry measurements.

Et_2O vapour diffusion into CH_3CN solutions of either **1** or **2** gave colourless single crystals of the appropriate di-solvate, $\mathbf{1}\cdot 2\text{CH}_3\text{CN}$ or $\mathbf{2}\cdot 2\text{CH}_3\text{CN}$ suitable for X-ray diffraction. The structure of $\mathbf{1}\cdot 2\text{CH}_3\text{CN}$ shows a pseudo octahedral metal center the two benzyl-protected pyrazolyl rings trans- to each other, Fig. 3. The Fe–N bond distance associated with the confused pyrazolyl (Fe–N2, 2.006(1) Å) is longer than those with the regular pyrazolyls (Fe–N11, 1.974(1) and Fe–N21, 1.975(1) Å). The average Fe–N distance of 1.985(1) Å is consistent with LS Fe(II). Finally, as shown in Fig. S7,[±] the supramolecular structure shows sheets of **1** parallel with the bc-plane stacked along the a-axis so as to form channels along c-where solvated CH_3CN molecules reside. Presumably, the weak van der Waals forces associated with these molecules permits the solvent to be easily removed under application of vacuum. Unfortunately, attempts to

obtain structures at higher temperatures were thwarted by weak diffraction, disorder of solvent and benzyl rings that seriously compromised quality below publication standards.

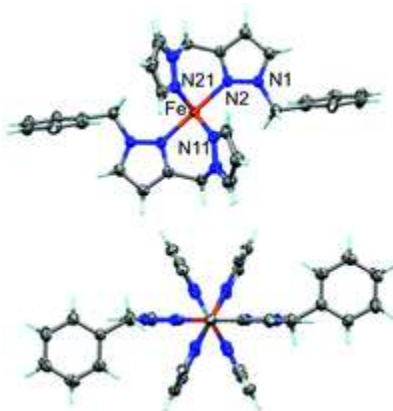


Fig. 3 Two views of the solid state structure of the dication in **1**·2CH₃CN. Thermal ellipsoids shown at 30% probability.

The structure of **2**·2CH₃CN at 100 K (Fig. S8 \pm) shows an average Fe–N distance of 2.214(1) Å that is in accord with HS Fe(II). Again, the Fe–N bond associated with the confused pyrazolyl is significantly longer than the other two on the same ligand (2.406(1) versus 2.112(1) and 2.123(1) Å) and is trans- to the same ring on the other ligand bound to iron. The larger steric bulk of the tosyl versus benzyl causes greater pyrazolyl ring twisting in the former (avg. FeN–NC_{methine} = 8.3° versus 3.8° for **1**·2CH₃CN), presumably hindering spin crossover.

The spin crossover behaviour of a sample of solid **1**·2CH₃CN freshly crystallized, decanted, and dried under a N₂ stream (to minimize solvent loss by vacuum drying) was interrogated by SQUID magnetometry over the temperature range 2 to 300 K (Fig. 4). The sample is clearly HS from 300 K to about 175 K with $\mu_{\text{eff}} = 5.1\mu_{\text{B}}$. Below 175 K the sample undergoes a gradual spin state change and reaches a minimum effective moment of $\mu_{\text{eff}} = 1.7\mu_{\text{B}}$ at 60 K. This residual moment differs from the typical value of 0.7 μ_{B} of iron(II) scorpionates (see Fig. 2) that arises from temperature independent paramagnetism (2nd order Zeeman effect on paramagnetism). Since the data were identical regardless of heating/cooling rates thus the HS state is not kinetically trapped,²⁶ we attribute the excess moment (ca.

$1\mu_B$) of the analytically pure sample to about a 7–10% HS Fe(II) that arises due either to unavoidable desolvation during drying and transfer to the magnetometer, to a portion of a yet-to-be-identified cis-isomer that may not undergo SCO, or to both. We favour the former given the variability in data when samples are subjected to different evacuation and handling procedures (Fig. S9 \pm). Regardless, the magnetic properties of $\mathbf{1}\cdot 2\text{CH}_3\text{CN}$ are clearly different than its desolvated counterpart $\mathbf{1}$ at low temperature and provide yet another example that solvate molecules can have a profound impact on SCO behaviour. The data are also significant as they demonstrate only the second example of SCO behaviour in a scorpionate that has a pyrazolyl substituent larger than a methyl proximal (β -) to the metal centre.

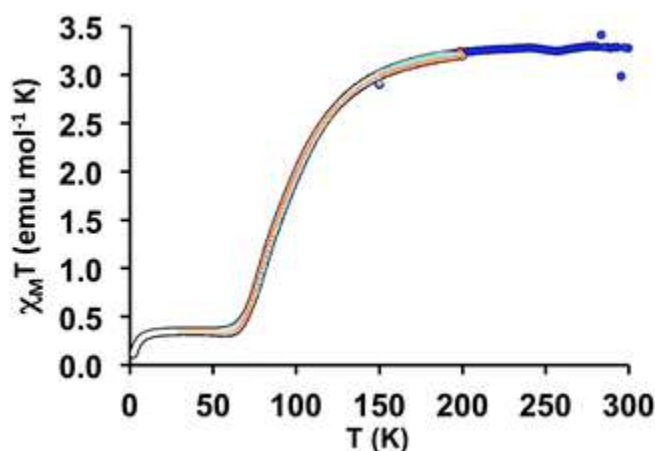


Fig. 4 Variable temperature magnetic data for $\mathbf{1}\cdot 2\text{CH}_3\text{CN}$. Key: Blue and light blue, first and second cooling cycle; red and orange, first and second heating cycle.

In summary, we have developed a multigram synthesis of the first example of a class of N-confused scorpionate ligand. In this first example, one pyrazolyl of a tris(pyrazolyl)methane is tethered to the sp^3 -methine carbon via a carbon rather than via the nitrogen of the heterocycle. One can envision other examples where two or all three pyrazolyls are connected to the methine carbon (or to a boron centre) in this fashion. This new ligand design opens the door synthetically to a wealth of nitrogen protection/deprotection reactions that could allow easy modification of the steric and electronic properties about the metals' first and second coordination sphere. In the current case we have altered one β -pyrazolyl substituent of the ligand (on the exo-N) to be an H, Bn, or Ts group. Each gave $[\text{Fe}(\text{X}L)_2]^{2+}$ complexes, thereby

showing a steric limit to such homoleptic moieties has not been breached by these small to modest-size groups. The electronic properties of these ligands compare favourably with both Tp and Tpm based scorpionates. The complexes $[\text{Fe}(\text{xL})_2](\text{BF}_4)_2$ exhibit a range of magnetic behaviour with the case of $x = \text{H}$ showing SCO behaviour near room temperature and above, in contrast to those with larger groups, $x = \text{Bn}$ or Ts , that remain high spin. The derivative $x = \text{Bn}$ can be induced to show SCO behaviour (with $T_{1/2}$ ca. 90 K) by crystallization with acetonitrile. It is hypothesized that the crystal packing in the solvate is such that the pyrazolyl rings are free to relax to give shorter Fe–N bonds and lower ring twisting associated with LS Fe(II) but the solvent-free complex may be more tightly packed and have more twisted pyrazolyl rings that prevents SCO behaviour. Unfortunately, the high mp of CH_3CN (225 K) precludes observation of SCO of **1** in solution (which may be expected to occur near 90 K, similar to the solid). The details of full structural investigations to test the above hypothesis and to delineate solvent and anion effects will be reported in due course. The reaction chemistry of metal complexes based on these and other, bulkier derivatives will be described elsewhere.

Notes and references

- ¹Selected reviews: S. Hayami, S. M. Holmes and M. A. Halcrow, *J. Mater. Chem. C*, 2015, 3, 7775–7778 Spin-Crossover Materials: Properties and Applications, ed. Malcolm A. Halcrow, John Wiley & Sons, Ltd., West Sussex, 2013; M. A. Halcrow, *Chem. Soc. Rev.*, 2011, 40, 4119–4142; G. J. Long, F. Grandjean and D. L. Reger, *Top. Curr. Chem.*, 2004, 233, 91–122 . Spin crossover in transition metal compounds II P. Gülich and H. A. Goodwin, *Top. Curr. Chem.*, 2004, 234, 1–47.
- ²O. Kahn and C. J. Martinez, *Science*, 1998, 279, 44–48.
- ³R. G. Miller and S. Brooker, *Chem. Sci.*, 2016, 7, 2501–2505; G. Galle, D. Deldicque, J. Degert, T. Forestier, J.-F. Letard and E. Freysz, *Appl. Phys. Lett.*, 2010, 96, 041907/1; Z. Ni and M. P. Shores, *J. Am. Chem. Soc.*, 2009, 131, 32–33.
- ⁴I.-R. Jeon, J. G. Park, C. R. Haney and T. D. Harris, *Chem. Sci.*, 2014, 5, 2461–2465; R. N. Muller, L. Van der Elst and S. Laurent, *J. Am. Chem. Soc.*, 2003, 125, 8405–8407.
- ⁵J. Huang, R. Xie, W. Wang, Q. Li and J. Yang, *Nanoscale*, 2016, 8, 609–616; M. Bernien, H. Naggert, L. M. Arruda, L. Kippen, F. Nickel, J. Miguel, C.

- F. Hermanns, A. Krüger, D. Krüger, E. Schierle, E. Weschke, F. Tuczek and W. Kuch, *ACS Nano*, 2015, 9, 8960–8966.
- ⁶M. Gruber, V. Davesne, M. Bowen, S. Boukari, E. Beaurepaire, W. Wulfhekel and T. Miyamachi, *Phys. Rev. B: Condens. Matter*, 2014, 89, 195415; T. Miyamachi, M. Gruber, V. Davesne, M. Bowen, S. Boukari, L. Joly, F. Scheurer, G. Rogez, T. K. Yamada, P. Ohresser, E. Beaurepaire and W. Wulfhekel, *Nat. Commun.*, 2012, 938, 1–6; T. G. Gopakumar, F. Matino, H. Naggert, A. Bannwarth, F. Tuczek and R. Berndt, *Angew. Chem., Int. Ed.*, 2012, 51, 6262–6266; M. S. Alam, M. Stocker, K. Gieb, P. Müller, M. Haryono, K. Student and A. Grohmann, *Angew. Chem., Int. Ed.*, 2010, 49, 1159–1163; A. Bousseksou, G. Molnár, P. Demont and J. Menegotto, *J. Mater. Chem.*, 2003, 13, 2069–2071.
- ⁷D. L. Reger, J. R. Gardinier, J. D. Elgin, M. D. Smith, D. Hautot, G. J. Long and F. Grandjean, *Inorg. Chem.*, 2006, 45, 8862–8875.
- ⁸L. G. Lavrenova and O. G. Shakirova, *Eur. J. Inorg. Chem.*, 2013, 670–682.
- ⁹S. E. Creutz and J. C. Peters, *Inorg. Chem.*, 2016, 55, 3894–3906; I. Kuzu, I. Krummenacher, I. J. Hewitt, Y. Lan, V. Mereacre, A. K. Powell, P. Höfer, J. Harmer and F. Breher, *Chem. – Eur. J.*, 2009, 15, 4350–4365.
- ¹⁰J. P. Jesson, S. Trofimenko and D. R. Eaton, *J. Am. Chem. Soc.*, 1967, 89, 3158–3167; G. J. Long and B. B. Hutchinson, *Inorg. Chem.*, 1987, 26, 608–613; F. Grandjean, G. J. Long, B. B. Hutchinson, L. Ohlhausen, P. Neill and J. D. Holcomb, *Inorg. Chem.*, 1989, 28, 4406–4414.
- ¹¹L. Salmon, G. Molnár, S. Cobo, P. Oulié, M. Etienne, T. Mahfoud, P. Demont, A. Eguchi, H. Watanabe, K. Tanaka and A. Bousseksou, *New J. Chem.*, 2009, 33, 1283–1289.
- ¹²T. Mahfoud, G. Molnár, S. Cobo, L. Salmon, C. Thibault, C. Vieu, P. Demont and A. Bousseksou, *Appl. Phys. Lett.*, 2011, 99, 053307.
- ¹³J. D. Oliver, D. F. Mullica, B. B. Hutchinson and W. O. Milligan, *Inorg. Chem.*, 1980, 19, 165–169; D. C. L. De Alwis and F. A. Schultz, *Inorg. Chem.*, 2003, 42, 3616–3622.
- ¹⁴H. Winkler, A. X. Trautwein and H. Toftlund, *Hyperfine Interact.*, 1992, 70, 1083–1086.
- ¹⁵J. J. McGarvey, H. Toftlund, A. H. R. Al-Obaidi, K. P. Taylor and S. E. J. Bell, *Inorg. Chem.*, 1993, 32, 2469–2412.
- ¹⁶P. Anderson, T. Astley, M. Hitchman, F. Keene, B. Moubaraki, K. S. Murray, B. Skelton, E. Tiekink, H. Toftlund and A. White, *J. Chem. Soc., Dalton Trans.*, 2000, 3505–3512.
- ¹⁷D. L. Reger, C. A. Little, A. L. Rheingold, M. Lam, L. M. Liable-Sands, B. Rhagitan, T. Concolino, A. Mohan, G. J. Long, V. Briois and F. Grandjean, *Inorg. Chem.*, 2001, 40, 1508–1520; V. Briois, P. Saintavit, G. J. Long and F. Grandjean, *Inorg. Chem.*, 2001, 40, 91–98.

- ¹⁸D. L. Reger, C. A. Little, V. G. Young Jr. and M. Pink, *Inorg. Chem.*, 2001, 40, 2870–2874.
- ¹⁹B. Moubaraki, B. A. Leita, G. J. Halder, S. R. Batten, P. Jensen, J. P. Smith, J. D. Cashion, C. J. Kepert, J.-F. Létard and K. S. Murray, *Dalton Trans.*, 2007, 4413–4426.
- ²⁰H. Park, J. S. Baus, S. V. Lindeman and A. T. Fiedler, *Inorg. Chem.*, 2011, 50, 11978–11989.
- ²¹P. Checchi, M. Berrettoni, M. Giorgetti, G. G. Lobbia, S. Calogero and L. Stievano, *Inorg. Chim. Acta*, 2001, 318, 67–76; D. M. Eichorn and W. H. Armstrong, *Inorg. Chem.*, 1990, 29, 3607–3612.
- ²²M. A. Goodman, A. Y. Nazarenko, B. J. Casavant, Z. Li, W. W. Brennessel, M. J. DeMarco, G. Long and M. S. Goodman, *Inorg. Chem.*, 2012, 51, 1084–1093 .
- ²³S. M. Allin, W. R. S. Barton, W. R. Bowman, E. Bridge, M. R. J. Elsegood, T. McInally and V. McKee, *Tetrahedron*, 2008, 64, 7745–7758.
- ²⁴K. I. Thé and L. K. Peterson, *Can. J. Chem.*, 1973, 51, 422–426; K. I. Thé, L. K. Peterson and E. Kiehlmann, *Can. J. Chem.*, 1973, 51, 2448–2451; L. K. Peterson, E. Kiehlmann, A. R. Sanger and K. I. Thé, *Can. J. Chem.*, 1974, 52, 2367–2374.
- ²⁵O. G. Shakirova, L. G. Lavrenova, A. S. Bogomyakov, K. Yu. Zhizhin and N. T. Kuznetsov, *Russ. J. Inorg. Chem.*, 2015, 60, 786–789; L. G. Lavrenova, A. D. Strekalova, A. V. Virovets, D. A. Piryazev, V. A. Daletskii, L. A. Sheludyakova, T. F. Mikhailovskaya and S. F. Vasilevskii, *Russ. J. Coord. Chem.*, 2012, 38, 507–514; L. G. Lavrenova, A. V. Virovets, E. V. Peresyphkina, A. D. Strekalova, D. A. Piryazev, V. A. Daletsky, L. A. Sheludyakova and S. F. Vasilevsky, *Inorg. Chim. Acta*, 2012, 382, 1–5.
- ²⁶G. Ritter, E. Koenig, W. Irlner and H. A. Goodwin, *Inorg. Chem.*, 1978, 17, 224–228.

Footnotes

† This paper is dedicated to Prof. Dan Reger on the occasion of his retirement.

‡ Electronic supplementary information (ESI) available: Experimental procedures, crystal data, other characterization data. CCDC [1478564](#), [1478566](#) and [1478567](#) for **1**·2CH₃CN, **2**·CH₃CN and **3**. For ESI and crystallographic data in CIF or other electronic format see DOI: [10.1039/c6dt01898j](#)